

Effects of Charge Impurities and Laser Energy on Raman Spectra of Graphene

Martin Hulman,^{*,†,‡} Miroslav Haluška,^{§,||} Giusy Scalia,^{§,⊥} Dirk Obergfell,[§] and Siegmar Roth[§]

Danubia NanoTech, s.r.o., Ilkovičova 3, 812 19 Bratislava, Slovakia, Austrian Research Centers, A-2444 Seibersdorf, Austria, Max-Planck Institut für Festkörperforschung, Heisenbergstr.1, Stuttgart, Germany, Micro- and Nano- Scale Engineering, Department of Mechanical Engineering, Eindhoven University of Technology, Eindhoven, The Netherlands, and ENEA C.R. Portici, Portici, Italy

Received May 20, 2008; Revised Manuscript Received September 9, 2008

ABSTRACT

The position and width of the Raman G-line was analyzed for unintentionally doped single-layered graphene samples. Results indicate a significant heating of the monolayer by the laser beam. Moreover, a weak additional component was resolved in the G-band. The position of the line is independent of the level of doping of the sample. We conclude that this new component is due to the phonons coupled to the intraband electronic transitions.

For a long time, graphene, a single layer of graphite, has been a tool for theoreticians to explain properties of bulk graphite or carbon nanotubes, never assuming that such a material could be prepared. A few years ago, graphene came into real life and since then has attracted considerable, increasing interest in condensed matter physics,^{1–3} the main reason being the electronic structure consisting of linear electronic bands around the Fermi level (for review of the electronic properties of graphene, see ref 4). Electrons behave like massless particles whose dynamics are governed by the Dirac equation. High electronic mobility^{5,6} and the observability of the quantum Hall effect⁷ even at room temperature⁸ make graphene an interesting candidate for nanoelectronics.

Like for carbon nanotubes, which can be regarded as rolled-up graphene layers, Raman spectroscopy has been the first choice for characterization of graphene samples. The high-energy second-order D* (referred to by some authors as 2D) line at about 2650 cm⁻¹ was used to resolve single-layer graphene samples.⁹ The shape, the width, and the position of this peak reflect the electronic band structure which is, in turn, dependent on the number of layers. This is because the double-resonance mechanism responsible for the D* line probes the splitting of the electronic band caused by the stacking of the graphene layers.

The doping state of a graphene layer can be traced with the help of the G-line ($\nu \sim 1582$ cm⁻¹).^{10,11} Both the line position and the line width show sensitivity to the shift of the Fermi level, ϵ_F , with respect to the charge-neutral Dirac points. Changes of the G-band induced by doping can only be correctly accounted for by assuming a violation of the adiabatic Born–Oppenheimer approximation.^{10,12,13} Considering the phonons as a static perturbation (adiabatic picture) leads to the phonon softening upon doping, which is not consistent with the experiments. When the free carrier density, n , is low and the condition $\nu > 2|\epsilon_F|$ holds, the G-band phonons may decay into electron–hole pairs. Then the width of the G-line broadens considerably and $d\nu/dn < 0$. If instead $\nu < 2|\epsilon_F|$, the Pauli principle forbids the phonon decay and only virtual electron–hole pairs can be created. The line gets narrow, and its width is eventually independent of doping. The phonon energy is still renormalized by the polarization of the electronic system, and $d\nu/dn > 0$.

A common feature of graphene layers, which can be derived from their Raman spectra, is the inhomogeneity of the charge distribution. This was considered as the origin of the observed changes in position and line width of the G-band. In fact, graphene may be unintentionally doped by gas molecules from the environment causing depletion of electrons from the sample. The G-line position varies even within the same graphene layer^{14,15} and its width may be considerably increased when the characteristic size of the charged domains becomes comparable to or smaller than the laser spot diameter.¹⁶

* Corresponding author, hulman@danubiananotech.com.

† Danubia NanoTech, s.r.o.

‡ Austrian Research Centers.

§ Max-Planck Institut für Festkörperforschung.

|| Eindhoven University of Technology.

⊥ ENEA C.R. Portici.

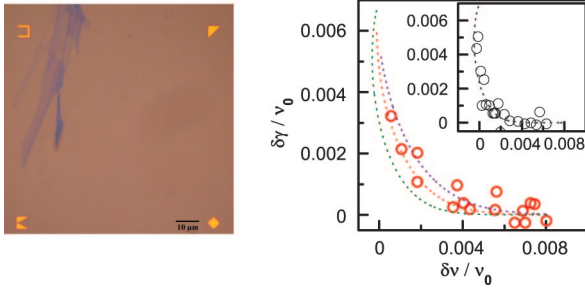


Figure 1. (left panel) Optical microscopy image of an ensemble of graphene flakes used for Raman measurements. The thickness of the flakes varies from a single to multiple layers (single, longish layer at the upper, left-hand side). Bright spots are the markers for identifying the position of the flake. (right panel) Relation between the width and the shift of the G-line in graphene for several different samples (circles). Here, $\gamma = \gamma_{\text{exp}} - \gamma'$, where γ_{exp} is the experimental line width and $\gamma' = 7.5 \text{ cm}^{-1}$. Similarly, $\delta\nu = \nu - \nu_0$ and $\nu_0 = 1583 \text{ cm}^{-1}$ were taken for the position of the G-band in the charge neutral (undoped) state. Theoretical curves are shown as dotted lines for temperatures of 300, 470, and 600 K (from bottom to top). The inset shows the same relation for data taken from ref 11 (points) and the theoretical curve for a temperature of 240 K. Here, the values of 6.6 cm^{-1} and 1584 cm^{-1} were set for γ' and ν_0 , respectively.

In all existing experimental work on graphene, laser powers in the milliwatt range were employed and regarded low enough to avoid any heating of the samples. This premise has never been questioned in the literature so far. Instead, the charge inhomogeneity was assumed as the most likely source of any discrepancy between experiments and theory. In this paper, we present results of Raman scattering experiments performed on single-layer graphene samples that contradict this common assumption. Analyzing the width and the position of the G-line, we show that the electronic system is significantly heated up by the incident laser light. Our experimental results can be properly explained only when the temperature is taken into account as a free parameter. Moreover, we observed a low-intensity satellite peak in addition to the main line in the G-band. Unlike the latter, the position of the satellite is, in fact, characteristic of the undoped sample. We argue that this line, previously not reported, is due to the phonons inducing intraband electronic transitions.

Graphene flakes were prepared following the procedures described in ref 1. Si/SiO₂ (300 nm Si oxide) chips were cleaned by ultrasonic treatment in acetone and isopropanol, followed by a 60 s oxygen plasma at 0.3 Torr and 200 W. Graphene and few-layer graphite flakes were prepared by distributing HOPG material onto a strip of Nitto tape and subsequently pressing the tape with the adhered graphite flakes onto the cleaned chips. The chips were equipped with geometrical markers for unambiguous identification of the sample's position. Monolayers of graphite, giving rise to a faint contrast in optical microscopy, were found with an optical microscope, as shown in the left panel of Figure 1. All the Raman measurements were performed with a Jobin Yvon-LabRam microscope system equipped with a 100× microscope at ambient conditions. The spectra were excited with a laser of 633 nm wavelength and a laser power of

~0.4 mW. Single-layered flakes were identified via the shape of the Raman D*-line.⁹

The Fermi level shift is not known in our experiments. It is therefore reasonable to directly relate the measured quantities in order to turn ϵ_F from an independent variable to a parameter this way. Such a relation for the position and the width of the G-line is shown in the right panel of Figure 1. Different graphene samples were analyzed for obtaining the experimental points shown in the figure. Note that, in all cases, the values in the plot were obtained by fitting the G-bands with a single Lorentz line only, thus avoiding overlap of G-lines coming from unequally doped domains. In addition, as the presence of a D-line can be correlated to defects present in the layer, which may, to some extent, mimic the influence of the doping,¹⁷ only spectra without D-lines were included.

In the plot, charge density increases from the upper left to the lower right corner. The G-band gets narrower and shifts to higher wave numbers as the Fermi level is moved away from the Dirac points. The lines acquire a finite width of about 7.5 cm^{-1} at high doping stages. This number appears somehow universal since very similar values were also found by other groups.^{10,11,16} The experimental points in Figure 1 exhibit substantial scattering, largely due to the error in determining the line widths. The error is estimated to be about $\pm 1 \text{ cm}^{-1}$, thus being most pronounced for the high doping levels.

Explicit formulas for the line width, γ , and the line shift, $\delta\nu$, of the G-band as a function of the Fermi level shift are given in refs 11 and 12. For the temperature-dependent line width we have

$$\gamma/\nu_0 = \frac{\pi\alpha}{2} \frac{\sinh(1/\tilde{T})}{\cosh(2\tilde{\epsilon}/\tilde{T}) + \cosh(1/\tilde{T})} \quad (1)$$

where we introduce the dimensionless quantities $\tilde{\epsilon} = |\epsilon_F|/h\nu_0$ and $\tilde{T}^{-1} = h\nu_0/2k_B T$. The position of the G-band in the absence of any doping is ν_0 and T is the temperature. The symbols k_B , h , and c have their usual meaning, being the Boltzmann and Planck constants and the speed of light, respectively. When $|\epsilon_F| \neq h\nu_0/2$, the line shift is only weakly temperature dependent, and for $T = 0$ it reads

$$\delta\nu/\nu_0 = (\nu - \nu_0)/\nu_0 = \alpha \left(\tilde{\epsilon} + \ln \left| \frac{1 - \frac{1}{2\tilde{\epsilon}}}{1 + \frac{1}{2\tilde{\epsilon}}} \right| \right) \quad (2)$$

where $\alpha = 4.43 \times 10^{-3}$. After eliminating ϵ_F from eq 1 and inserting it in eq 2, the line width becomes a function of the line shift. The calculated line width of the G-band as a function of its position is shown in Figure 1 with dashed lines corresponding to three different temperatures. Contrary to expectations, the theory does not reproduce the measurements satisfactorily when $T = 300 \text{ K}$. The deviation is most pronounced for the samples with lower levels of doping. The best agreement was obtained when the temperature was raised to about 470 K. Despite of the fact that the laser power was kept in the milliwatt range, this temperature is unexpectedly high and points to substantial heating of the electronic system by the incident laser light during the measurements.

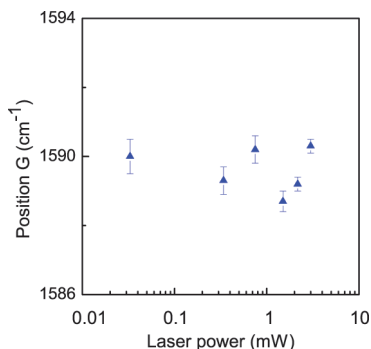


Figure 2. The dependence of the G-band position on the power of the exciting laser.

Unfortunately, we do not know the actual temperature of the samples from an independent measurement.

To corroborate further our findings, we analyzed the measurements of ref 11 in the same way. They were conducted at 10 K. The line width was systematically larger than that predicted from theory for 10 K. Yan et al. attributed the observed deviations to the inhomogeneities in the charge density. While the latter may indeed contribute, we allowed the temperature to change and used it as a free parameter in our analysis. In this way we obtained an excellent fit between the experiment and theory for a temperature of 240 K. This higher temperature also minimizes the differences in line positions measured from unequally charged domains and the overall result is a single Raman line, in agreement with the experiments. The results are summarized in the inset of Figure 1.

The significant heating of electrons photoexcited by laser pulses was recently discussed theoretically for graphene¹⁹ and studied experimentally for very thin graphite flakes.²⁰ The electrons relax back to the ground state emitting high-energy optical phonons. Calculations demonstrated that such a hot phononic ensemble contains mainly $\mathbf{k} \neq 0$ phonons and that the in-center G ones are only marginally affected by the raised electronic temperature. We have experimentally verified this conclusion by measuring the position of the G-band as a function of the laser power. The results are displayed in Figure 2. The spectra were taken after the sample had been annealed at 150 °C in Ar atmosphere eliminating those volatile dopants which could be removed from the graphene surface by the laser beam. Therefore, we can reasonably assume that the level of doping did not change during the Raman measurement. The sample still remained doped, as seen from the position of the G-line at 1590 cm⁻¹ for the lowest laser power. As demonstrated in Figure 2, there is a weak influence of the laser power on the position of the G-line. In any case, the temperature dependence is completely different from the linear downshift of the G-line observed for a graphene sample heated by a hot stage.²¹ Therefore, we may conclude that the G-phonons are indeed not heated by the laser beam.

Among many obtained spectra, there is a subset which shows a small shoulder on the low-energy side of the main G-peak (referred to as G₁ thereafter). Examples of such spectra from different samples are shown in Figure 3 where

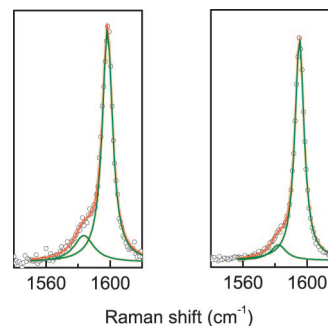


Figure 3. The G-band spectra (circles) showing the weak G₂ components of the band in addition to the dominating G₁ components (green solid lines).

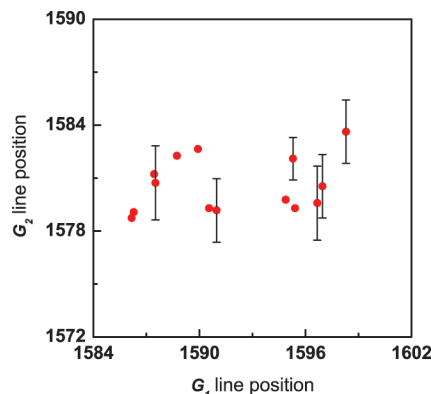


Figure 4. The shift of the G₂ component as a function of the doping level represented here by the charge-induced shift of the G₁ component. The position of G₂ is clearly independent of doping.

the shoulders have been resolved as weak lines (referred to as G₂). The important feature of the latter is their always smaller intensity compared to the main G₁ peak. This indicates that this feature is likely not a consequence of inhomogeneous doping, since in such a case the lines would have a strongly varying intensity. Interestingly, the positions of the weak lines do not change irrespective of the position of the strong ones. This is demonstrated in Figure 4 in more detail. As before, the position of the G₁ components changes according to the doping level while that of the G₂ ones fluctuates around 1581 cm⁻¹. Since the charge-induced shift is due to the interaction of the G-phonons with electrons, this indicates that the G₁- and G₂-phonons interact differently as discussed below.

When the electronic system is considered, graphene comprises properties of both a metal and a semiconductor. Therefore, in addition to the interband transitions discussed in refs 10–12, intraband transitions also contribute to the polarization of the electronic system.¹³ The principal difference between these two processes is reflected in the dependence of the electronic susceptibility on the momentum of the electron–hole excitation, q . For interband transitions, the susceptibility is momentum independent for $q \rightarrow 0$ whereas it vanishes for the intraband ones in the same limit. For a translationally invariant system, the long-wavelength G-phonons create electron–hole pairs with $q = 0$ thus contributing to the interband susceptibility only. When the translational symmetry is broken, the condition for q is

relaxed and the electron–hole pairs within the same electronic band can also be created. Therefore, G-phonons may simultaneously induce interband as well as intraband electronic transitions.

For the latter, the charge induced shift of the G-phonon energy becomes q dependent. Specifically, it was shown that $\delta\nu \sim (qa)^2$, where $a = 1.42 \text{ \AA}$, is the carbon–carbon distance.¹³ If $1/q$ acts as a characteristic length describing the disorder or the finite size of the sample, it is reasonable to assume that $aq \ll 1$. As a consequence, the q -dependent factor makes the G-line shift very small due to the intraband transitions. Note that both the inter- and intraband transitions have an identical $n^{1/2}$ dependence of the charge-induced shift on the charge concentration.

From the above facts, the following scenario emerges. At low doping stages, the shift of both G-line components is small and the width is the largest. Therefore, a single Raman line is observed in the spectrum. As doping increases, the component whose energy is renormalized due to the interband transitions is blue-shifted while the other one stays at the same position as for an undoped sample. Eventually, a single G-line splits into two components. This is in agreement with our observation, and we ascribe the G_1 and G_2 components of the G-band to phonons coupling to the interband and intraband electronic transitions, respectively. The weak intensity of the G_2 component can likely be related to the smaller probability of the phonon-induced intraband transitions as compared to the interband ones. The scattering of the experimental points in Figure 4 is due to uncertainties in the determination of the line positions of the weak lines which are in a close proximity to the strong ones.

In summary, we discussed two new observations regarding Raman measurements of graphene monolayers. First, we reinterpreted the charge-induced changes of the width and position of the G-line in terms of the influence of temperature. We showed that the incident laser beam heats up the layer far beyond previous expectations. On the other hand, the heating is restricted to the electronic system only, without influencing directly the long-wavelength G-phonons in the Raman spectra. This might be the reason why this effect has been overlooked so far. Second, we detected a weak component in the G-band in addition to the major line. Besides the remarkable difference in the intensity, the most significant distinction between the lines is the unsusceptibility of the weaker one to doping. We ascribed this line to the

G-band phonons coupled to the intraband electronic transitions, in accordance with the theoretical predictions.

Acknowledgment. M.H. and M.H. acknowledge support from the Slovak agency APVV under the project no. 06-628. G.S. thanks the Marie Curie Intra- European Fellowship with Contract MEIF-CT-2005-025934 for financial support. We also acknowledge Mr. Armin Schulz (MPI Stuttgart) for technical assistance with Raman experiments.

References

- (1) Novoselov, K. S.; Jiang, D.; Schedin, F.; Booth, T. J.; Khotkevich, V. V.; Morozov, S. V.; Geim, A. K. *Proc. Natl. Acad. Sci. U.S.A.* **2005**, *102*, 10451.
- (2) Novoselov, K. S.; Geim, A. K.; Morozov, S. V.; Jiang, D.; Katsnelson, M. I.; Grigorieva, I. V.; Dubonos, S. V.; Firsov, A. A. *Nature* **2005**, *438*, 197.
- (3) Zhang, Y. B.; Tan, Y. W.; Stormer, H. L.; Kim, P. *Nature* **2005**, *438*, 201.
- (4) Castro Neto, A. H.; Guinea, F.; Peres, N. M. R.; Novoselov, K. S.; Geim, A. K. *Rev. Mod. Phys.*, in press.
- (5) Han, M. Y.; Ozyilmaz, B.; Zhang, Y. B.; Kim, P. *Phys. Rev. Lett.* **2007**, *98*, 206805.
- (6) Morozov, S. V.; Novoselov, K. S.; Katsnelson, M. I.; Schedin, F.; Elias, D. C.; Jaszczak, J. A.; Geim, A. K. *Phys. Rev. Lett.* **2008**, *100*, 016602.
- (7) Peres, N. M. R.; Guinea, F.; Castro Neto, A. H. *Phys. Rev.* **2006**, *B 73*, 125411.
- (8) Novoselov, K. S.; Jiang, Z.; Zhang, Y.; Morozov, S. V.; Stormer, H. L.; Zeitler, U.; Maan, J. C.; Boebinger, G. S.; Kim, P.; Geim, A. K. *Science* **2007**, *315*, 1379.
- (9) Ferrari, A. C.; Meyer, J. C.; Scardaci, V.; Casiraghi, C.; Lazzeri, M.; Mauri, F.; Piscanec, S.; Jiang, D.; Novoselov, K. S.; Roth, S.; Geim, A. K. *Phys. Rev. Lett.* **2006**, *97*, 187401.
- (10) Pisana, S.; Lazzeri, M.; Casiraghi, C.; Novoselov, K. S.; Geim, A. K.; Ferrari, A. C.; Mauri, F. *Nat. Mater.* **2007**, *6*, 198.
- (11) Yan, J.; Zhang, Y. B.; Kim, P.; Pinczuk, A. *Phys. Rev. Lett.* **2007**, *98*, 166802.
- (12) Lazzeri, M.; Mauri, F. *Phys. Rev. Lett.* **2006**, *97*, 266407.
- (13) Castro Neto, A. H.; Guinea, F. *Phys. Rev. B* **2007**, *75*, 045404.
- (14) Haluška, M.; Obergfell, D.; Meyer, J. C.; Scalia, G.; Ulbricht, G.; Krauss, B.; Chae, D. H.; Lohmann, T.; Lebert, M.; Kaempgen, M.; Hulman, M.; Smet, J.; Roth, S.; von Klitzing, K. *Phys. Status Solidi B* **2007**, *244*, 4143.
- (15) Stampfer, C.; Molitor, F.; Graf, D.; Ensslin, K.; Jungen, A.; Hierold, C.; Wirtz, L. *Appl. Phys. Lett.* **2007**, *91*, 241907.
- (16) Casiraghi, C.; Pisana, S.; Novoselov, K. S.; Geim, A. K.; Ferrari, A. C. *Appl. Phys. Lett.* **2007**, *91*, 233108.
- (17) Das, A.; Chakraborty, B.; Sood, A. K. cond-mat/07104160.
- (18) Das, A.; Pisana, S.; Piscanec, S.; Chakraborty, B.; Saha, S. K.; Waghmare, U. V.; Yang, R.; Krishnamurthy, H. R.; Geim, A. K.; Ferrari, A. C.; Sood, A. K. cond-mat/07091174.
- (19) Butscher, S.; Milde, F.; Hirtschulz, M.; Malic, E.; Knorr, A. *Appl. Phys. Lett.* **2007**, *91*, 203103.
- (20) Kampfrath, T.; Perfetti, L.; Schapper, F.; Frischkorn, C.; Wolf, M. *Phys. Rev. Lett.* **2005**, *95*, 187403.
- (21) Calizo, I.; Balandin, A. A.; Bao, W.; Miao, F.; Lau, C. N. *Nano Lett.* **2007**, *7*, 2645.

NL8014439